

Optical Engineering

OpticalEngineering.SPIEDigitalLibrary.org

Design of zoom homogenizer to control size of illumination field

Taeshin Kim
Seungjin Hwang
Kyung Hee Hong
Tae Jun Yu

Design of zoom homogenizer to control size of illumination field

Taeshin Kim,^a Seungjin Hwang,^a Kyung Hee Hong,^a and Tae Jun Yu^{a,b,*}

^aHandong Global University, Department of Advanced Green Energy and Environment, Pohang, Republic of Korea

^bHandong Global University, Global Institute of Laser Technology, Global Green Research and Development Center, Pohang, Republic of Korea

Abstract. We proposed a zoom homogenizer that can control the size of the illumination field by adding one lens array to the conventional imaging-type beam homogenizer. An equivalent lens system was used to derive the imaging condition and size of the illumination field. The result of the ray-tracing simulation shows the validity of the zoom homogenizer to generate the uniform and sharp-edged beam. We presented the strengths and weaknesses of the zoom homogenizer in terms of its etendue with the maximum acceptance angle of the system. © The Authors. Published by SPIE under a Creative Commons Attribution 3.0 Unported License. Distribution or reproduction of this work in whole or in part requires full attribution of the original publication, including its DOI. [DOI: 10.1117/1.OE.57.3.035102]

Keywords: beam homogenizers; beam shaping; zoom lenses; lens array; illumination engineering.

Paper 171329 received Aug. 23, 2017; accepted for publication Mar. 6, 2018; published online Mar. 24, 2018.

1 Introduction

A beam homogenizer, which is one of the beam-shaping methods, has been researched and developed. This method to make the uniform and sharp-edged beam has the advantage of high energy efficiency due to having no energy loss theoretically.¹ The output beam profile of the beam homogenizer is not significantly affected by the input beam condition such as size, shape, and distribution.^{2,3} Recently, the optimization research of the beam homogenizer have been performed to improve the output beam quality.⁴⁻⁶

The zoom function is also useful in many industrial applications. The zoom function changes the irradiated image size so the energy fluence or radiant intensity can be easily adjusted.⁷ The real-time control of these will be practical or useful in some situations.⁸ The conventional beam homogenizer can change the image size by moving the position of the lens array (LA). However, a sharp-edged beam cannot be obtained at all zoom positions.

There have been various studies by adding zoom function in beam homogenization technique to overcome this problem. Researchers have tried to realize the zoom function by modifying the conventional beam homogenizer itself⁹ or by adding the lenses to condenser lens part.¹⁰⁻¹³ Several researchers have added a zoom lens to the beam homogenizer and called it a zoom homogenizer.^{11,12} In general, zoom lens systems produce a clear image with a fixed image plane at all zoom positions.^{14,15} But they cannot generate a sharp-edged beam also the position of the image plane varies according to the change in the zoom positions.

In this study, we proposed a zoom homogenizer that can produce a sharp-edged beam at all zoom positions and have a fixed image plane. It was designed by adding an LA to the conventional beam homogenizer. The optical system was assumed as thin lenses, and the imaging condition was derived with equivalent focal length. We confirmed the validity of the proposed method by performing ray-tracing simulation. We also analyzed the maximum angle of the

incident beam that the optical system could allow and presented the advantages and limitations of this system regarding the etendue.

2 Derivation of Illumination Field Size According to Zoom Positions

The conventional beam homogenizer can be divided into two types: nonimaging and imaging.^{16,17} The nonimaging type consists of a single LA and a single condenser lens (CL) [Fig. 1(a)]. As there is no imaging condition, a uniform but unclear image is acquired. In contrast, the imaging-type beam homogenizer consists of a pair of LAs and a CL [Fig. 1(b)]. The LA1 plays the role of an object whose image is relayed by the LA2 in the imaging condition.³ Note that marginal rays are only in Fig. 1(b), because the LA2 plays an aperture stop role in the imaging type.^{17,18} A uniform and sharp-edged image can be obtained at the image plane using this homogenizer type. In this study, we designed an imaging and zooming homogenizer by adding one LA to the conventional imaging-type beam homogenizer.

The zoom optical system implies a system in which the effective focal length (EFL) or the magnification continuously changes while the image plane is maintained.¹⁵ In the proposed optical system, the EFL (f_{LA}) of LAs is changed continuously, and the image plane is fixed to the focal length (f_c) of the CL. Figure 2(a) shows a zoom homogenizer with three LAs and one CL. For the collimated incident beam, the image plane is at a distance from f_c .

The use of an equivalent lens enables a complex optical system to be simplified using a lens approximation considered as a thin lens. The design using the equivalent lens is useful to derive the size of the illumination field of the imaging beam homogenizer at all zoom positions. Similar to that of the conventional imaging beam homogenizer, the size (D) of the illumination field of the zoom homogenizer is expressed as the ratio of the focal length (f_c) of CL and the EFL (f_{LA}) of LAs; the pitch size (p) of the LA is as follows:

$$\frac{D}{p} = \frac{f_c}{f_{LA}}. \quad (1)$$

*Address all correspondence to: Tae Jun Yu, E-mail: taejunyu@handong.edu

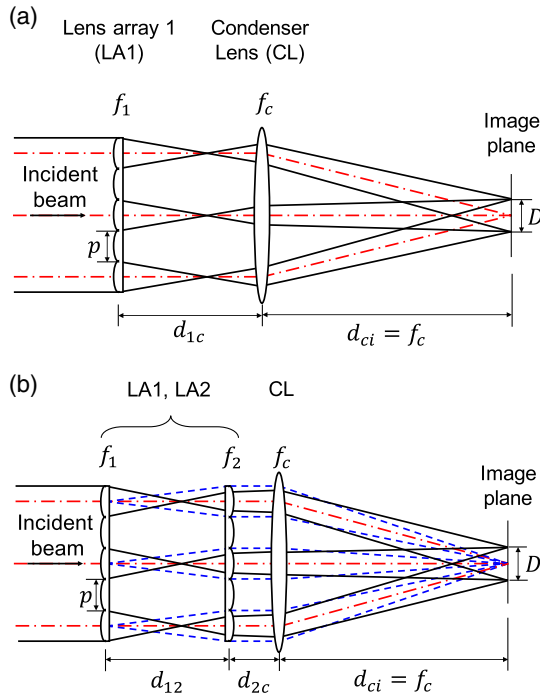


Fig. 1 Schematic structure of the beam homogenizer of (a) nonimaging type and (b) imaging type: black solid lines represent light rays, red dash-dotted lines represent central rays, and blue dashed lines represent marginal rays.

In this case, the EFL of three LAs can be written as¹⁹

$$f_{LA} = \frac{f_1 f_2 f_3}{f_1 f_2 + f_1 f_3 + f_2 f_3 - d_{12}(f_2 + f_3 - d_{23}) - d_{23}(f_1 + f_2)}, \quad (2)$$

where f_1 , f_2 , and f_3 are the focal lengths of LA1, LA2, and LA3, respectively, and d_{12} and d_{23} are the distances between LA1 and LA2 and LA2 and LA3, respectively.

Although there are several variables to determine the size of the illumination field, not every variable is involved in the imaging condition, under which the images of the LA1 lenslets are delivered and perfectly concentrated to the image plane to generate a sharp-edged beam. The key of the imaging condition in the beam homogenizer is to collimate the marginal rays passing through the edge of LA3, which plays the role of aperture stop in this system, to the CL. In a conventional imaging beam homogenizer, only one variable exists regarding the distance: d_{12} . As the imaging condition is fixed, that is, $d_{12} = f_2$,² zooming is impossible; however, this system comprises two variables regarding distance: d_{12} and d_{23} [Eq. (2)]. The determination of the imaging condition for this system can help in designing the zoom homogenizer.

To determine the imaging condition of the zoom homogenizer, we applied the method of the equivalent lens (Fig. 2). The green box in Fig. 2(b) displays the simplified lenslet system of LAs in Fig. 2(a). The marginal rays initiating from the center of LA1 are collimated using LA2 and LA3. Among the three LAs, LA2, and LA3 can be converted into one LA with focal length f_{23} , which can be written as

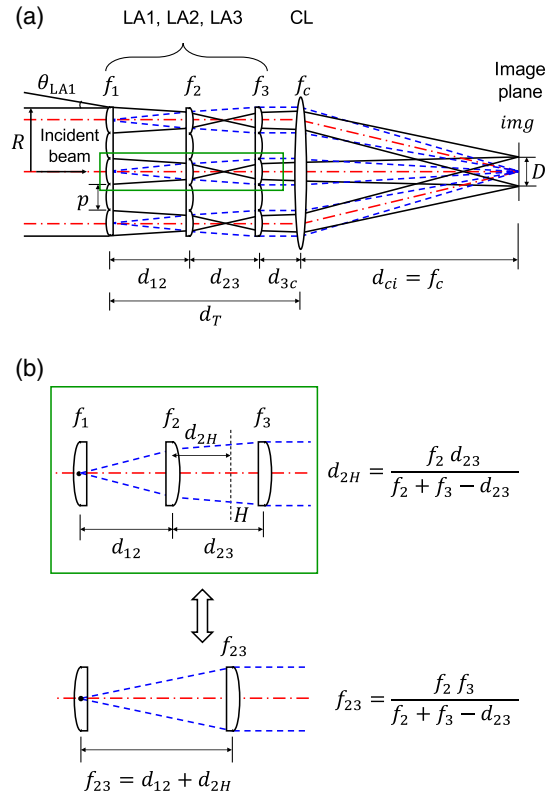


Fig. 2 (a) Schematic structure of the zoom homogenizer and three rays types: black solid lines represent light rays, red dash-dotted lines represent central rays, blue dashed lines represent marginal rays, and the green box represents the lenslet channel at the center of the LAs. (b) Equivalent lens system of LA2 and LA3 in the green box in Fig. 2(a).

$$f_{23} = \frac{f_2 f_3}{f_2 + f_3 - d_{23}}. \quad (3)$$

As f_2 and f_3 are equivalently converted to f_{23} , a principal plane H is formed between LA2 and LA3. The distance between LA2 and H , that is, d_{2H} can be written as

$$d_{2H} = \frac{f_2 d_{23}}{f_2 + f_3 - d_{23}}, \quad (4)$$

which determines the position of the equivalent lens of LA2 and LA3. As the equivalently converted focal length f_{23} is also expressed as $f_{23} = d_{12} + d_{2H}$, the substitution of Eqs. (3) and (4) in this equation leads to the derivation of the imaging condition

$$d_{12} = \frac{f_2(f_3 - d_{23})}{f_2 + f_3 - d_{23}}, \quad (5)$$

or

$$d_{23} = \frac{f_2 f_3 - d_{12}(f_2 + f_3)}{f_2 - d_{12}}. \quad (6)$$

Substituting Eq. (5) or Eq. (6) in Eqs. (1) and (2), we obtain the size of the illumination field in the imaging condition

$$D = \frac{pf_c f_2}{f_3(f_2 - d_{12})} = \frac{pf_c(f_2 + f_3 - d_{23})}{f_2 f_3} \quad (7)$$

Unlike the conventional beam homogenizer, the distance variables of the lenses are contained and coupled in the imaging condition of the zoom homogenizer. The size of the illumination field is simplified based on the imaging condition. Note that focal length (f_1) of LA1 illustrated as the dotted line in Fig. 2(b) is not involved in the imaging condition [Eq. (5) or Eq. (6)] as well as the size of the illumination field [Eq. (7)]. This is because, as mentioned earlier, LA1 plays the role of an object in the imaging condition.

A zoom ratio is the ratio of maximum EFL to the minimum EFL.¹⁵ The zoom ratio R_z is defined as

$$R_z = \frac{f_2 - d_{12,z3}}{f_2 - d_{12,z1}} = \frac{f_2 + f_3 - d_{23,z1}}{f_2 + f_3 - d_{23,z3}} \quad (8)$$

where subscripts $z1$ and $z3$ are the first and third zoom positions, respectively. To obtain high zoom ratio, it is advantageous to utilize small f_2 and f_3 or the highest difference between the distances of the first and third zoom positions.

3 Design Example of the Zoom Homogenizer in Case of $f_1 = f_2 = f_3$

3.1 Ray-Tracing Simulation

In Sec. 2, we derived the size of the zoom homogenizer in the imaging condition using the equivalent lens. This section also shows the result of the ray-tracing simulation conducted using the lens design program CODE V. Because the shape of the lenslets produces the shape of the illumination field at the image plane,² we have configured zoom homogenizer with the LAs, which have square-shaped lenslets in the simulation as a design example. Figure 3 shows the lens viewing

and spot diagrams in CODE V according to the zoom positions. The simulation parameters are shown in Table 1. For the simple simulation, f_1 , f_2 , and f_3 are all the same, that is, 60.0 mm. The distances between LAs, that is, d_{12} and d_{23} , satisfy the imaging condition. The zoom homogenizer was arranged as an inner zoom, in which the total length of the optical system is fixed (Fig. 3). LA2 and LA3 play the role of variator and compensator, respectively. The blue lines connected to LAs according to the zoom position present the zoom locus. The position of the image plane is fixed even though f_{LA} changes. However, the image size (D) of the illumination field changes, thus satisfying the image condition, Eq. (7), according to the zoom positions. Figure 3 shows a spot diagram at each zoom position with a sharp-edged square-shaped beam. According to the beam size (15.0 mm) at the second zoom position, when f_{LA} is minimum, the beam size is enlarged to 18.3 mm, and when f_{LA} is maximum, it reduced to 11.7 mm. The simulation result shows that the imaging condition in the zoom homogenizer is reliable. Furthermore, the zoom ratio is calculated using Eq. (8) and is ~ 1.6 .

Figure 4 shows the magnification and normalized energy fluence according to the change of d_{12} . The magnification is defined as the ratio of the size (D) of the illumination field at

Table 1 Parameters of the example simulation in (mm).

	$p = 3.0$	$f_{1,2,3} = 60.0$	$f_c = 200.0$	d_{12}	d_{23}	d_{3c}	$d_{ci} = f_c$	f_{LA}	D_z
Zoom1				27.3	10.0	32.7		32.7	18.3
Zoom2				20.0	30.0	20.0	200.0	40.0	15.0
Zoom3				8.6	50.0	11.4		51.4	11.7

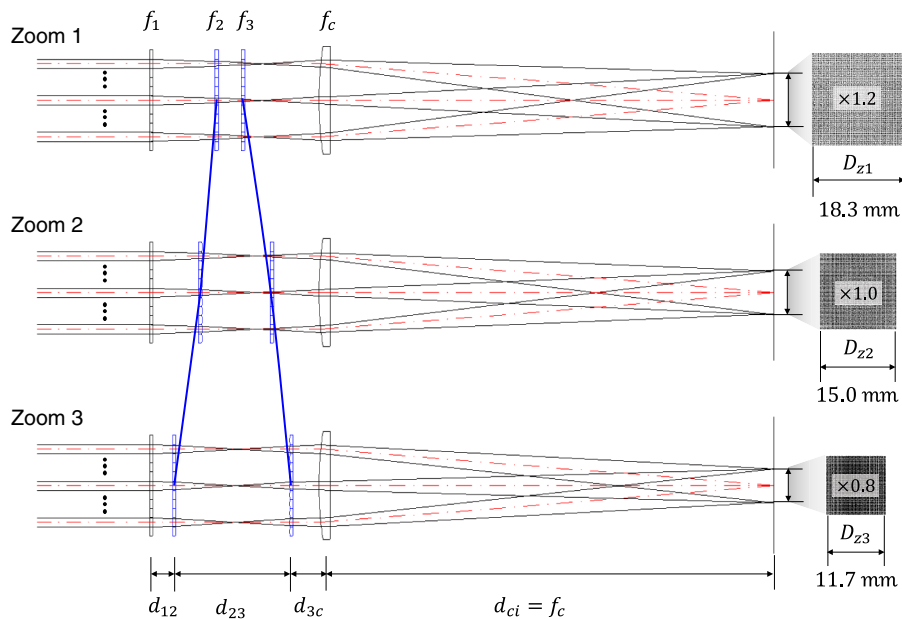


Fig. 3 Lens viewing and spot diagram of the design example of the imaging condition according to the zoom positions. The blue solid lines represent the zoom locus of the variator (LA2) and compensator (LA3).

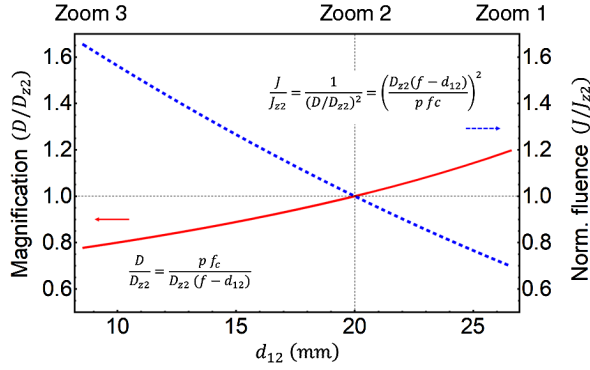


Fig. 4 The red solid line represents the relation between d_{12} and magnification, while the blue dashed line represents the relation between d_{12} and normalized fluence.

each zoom position to the size (D_{z2}) of the second zoom position. The maximum and minimum magnifications are ~ 1.2 and 0.8 at zoom1 and zoom3, respectively. The energy fluence, beam intensity, or radiated area are a more direct and important factor than the image size in the industrial field. As aforementioned, the normalized fluence is the ratio of energy fluence (J) at each zoom position to the energy fluence (J_{z2}) at the second zoom position. The maximum and minimum values of the normalized fluence are ~ 1.7 and 0.7 , respectively.

3.2 Pros and Cons of the Proposed System

In Secs. 2 and 3.1, we have assumed that the incident beam is parallel to the zoom homogenizer. But the incident beam may not be collimated or parallel to the zoom homogenizer in practical situations. The beamlets passing through the lenslet create a crosstalk that invades the adjacent area of the next LA. It happens when the incident beam has an angle that exceeds the etendue of the system.^{20,21} The etendue of the light source should be lower than the etendue of the system to prevent this kind of situation. We have analyzed the etendue of the system with the maximum acceptance angle, which occurs with no overflow at all zoom positions. The following system matrix gives the information of the angle and the image size at the image plane when the incident ray has an arbitrary angle.

$$\begin{pmatrix} \theta_{\text{img}} \\ h_{\text{img}} \end{pmatrix} = \begin{pmatrix} 1 & 0 \\ f_c & 1 \end{pmatrix} \begin{pmatrix} 1 & -\frac{1}{f_c} \\ 0 & 1 \end{pmatrix} \begin{pmatrix} 1 & 0 \\ d_{3c} & 1 \end{pmatrix} \\ \times \left[\begin{pmatrix} 0 \\ -np \end{pmatrix} + \begin{pmatrix} 1 & -\frac{1}{f_3} \\ 0 & 1 \end{pmatrix} \begin{pmatrix} 1 & 0 \\ d_{23} & 1 \end{pmatrix} \begin{pmatrix} 1 & -\frac{1}{f_2} \\ 0 & 1 \end{pmatrix} \right] \\ \times \begin{pmatrix} 1 & 0 \\ d_{12} & 1 \end{pmatrix} \begin{pmatrix} 1 & -\frac{1}{f_1} \\ 0 & 1 \end{pmatrix} \begin{pmatrix} \theta_{\text{LA1}} \\ h_{\text{LA1}} \end{pmatrix}. \quad (9)$$

In Eq. (9), θ_{LA1} and h_{LA1} are the angle and the height of the incident ray at LA1, respectively, and θ_{img} and h_{img} are the angle and the height of the image at the image plane, respectively. A local coordinator of the n 'th array $\Delta h = -np$ determines the position of the rays according to the lenslet channel. The ray height at the image plane, h_{img} , in imaging condition is

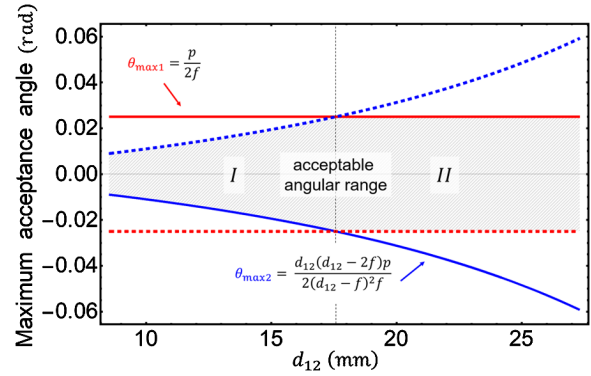


Fig. 5 Two cases of the maximum acceptance angle and the acceptable angular range of this setup: red and blue solid lines represent two cases, dashed lines represent the flipped lines of each colored line, and the hatched area represents the acceptable angular range along the zoom positions.

$$h_{\text{img}} = \frac{p f_c f_2}{2 f_3 (d_{12} - f_2)}, \quad (10)$$

and is a half of the image size (D) of Eq. (7). It is worth noting that h_{img} is not influenced by the incident angle to LA1, θ_{LA1} . It is valid in the thin lens approximation scheme.

We have to consider the cases of ray clipping by LA2 or LA3 to determine the maximum acceptance angle for the zoom homogenizer. In this system, two cases are significant (Fig. 5). The first case ($\theta_{\text{max}1}$) is that the incident ray, which has an angle starting from the upper edge ($p/2$) of LA1 hits the upper edge of the LA2. In this case, the angle corresponds to the numerical aperture of LAs (NA_{LA}) in common with the conventional beam homogenizer.²¹ Thus, it is a fixed value regardless of the zoom positions (red solid line). The second case ($\theta_{\text{max}2}$) is that the incident ray hits the lower edge ($-p/2$) of the LA3. The maximum angle varies as the zoom position changes in this case (blue solid line). These two cases are dominant, and they correspond to the maximum acceptance angles in this system. The other cases are not meaningful in this system.

The dashed lines in Fig. 5 mean mirrored values of each solid line, respectively, by considering the symmetry of the optic axis of the incoming ray. The pairs of the original line and the flipped line form the acceptable angular range. The case that has the smallest absolute angle has to be selected to define the angular limitation for this system among these cases. In other words, it is required to limit the zoom range when the angle of the input source is partially out of acceptable angular range.

The product of the angle θ_{img} and the height h_{img} of the ray is almost constant when $\theta_{\text{LA1}} = \theta_{\text{max}1}$, $n = 5$, and d_{12} is in zone II. Especially, it can become the etendue-conserving system of the output product ($\theta_{\text{img}} h_{\text{img}}$), which is the same as the input product ($R \cdot \text{NA}_{\text{LA}}$) when $d_T = f_c$.²¹

4 Conclusion

We have designed the zoom homogenizer using three LAs, and it is confirmed by using the ray-tracing simulation. The image size is changed continuously with having no variations in its image distance and its edge steepness. The zoom ratio was 1.6 in the design example, which is configured as an inner zoom with the same three LAs. The zoom

homogenizer works well in the acceptable angular range without a crosstalk in the LA system. It will be useful in many industrial applications, which are required to regulate the intensity or energy fluence with a sharp edge steepness.

Acknowledgments

This work was supported by the Industrial Strategic Technology development program, 10048964. The development of the 125 J-Hz laser system for laser peening was funded by the Ministry of Trade, Industry, and Energy (MI, Korea).

References

- O. Homburg et al., "Efficient beam shaping for high-power laser applications," *Proc. SPIE* **6216**, 621608 (2006).
- M. Zimmermann et al., "Microlens laser beam homogenizer: from theory to application," *Proc. SPIE* **6663**, 666302 (2007).
- R. Voelkel and K. J. Weible, "Laser beam homogenizing: limitations and constraints," *Proc. SPIE* **7102**, 71020J (2008).
- Z. Wang et al., "Analytical model of microlens array system homogenizer," *Opt. Laser Technol.* **75**, 214–220 (2015).
- Y. Jin, A. Hassan, and Y. Jiang, "Freeform microlens array homogenizer for excimer laser beam shaping," *Opt. Express* **24**, 24846–24858 (2016).
- S. Hwang et al., "Design of square-shaped beam homogenizer for petawatt-class Ti:sapphire amplifier," *Opt. Express* **25**, 9511–9520 (2017).
- B. Ehlers, "Industrial lasers: zoom optics maximize diode-laser efficiency," *Laser Focus World* **36**(2), 117–122 (2000).
- W. Todt, "Laser zoom optics enable real-time machining," *Laser Focus World* **50**(2), 10 (2014).
- J. M. Hoffman et al., "Zoom illumination system for use in photolithography," US Patent 6,307,682 (2001).
- D. M. Brown, "Variable ring beam integrators for product marking and machining," *Proc. SPIE* **4443**, 159–165 (2001).
- S. Bollanti, P. D. Lazzaro, and D. Murra, "More about the light beam shaping by the integration method," *Eur. Phys. J. Appl. Phys.* **28**(2), 179–186 (2004).
- S. Bollanti, P. D. Lazzaro, and D. Murra, "Performance of a zoom homogenizer for reshaping coherent laser beams," *Opt. Commun.* **264**(1), 174–179 (2006).
- R. Wu et al., "Freeform lens arrays for off-axis illumination in an optical lithography system," *Appl. Opt.* **50**, 725–732 (2011).
- A. Mikš, J. Novák, and P. Novák, "Method of zoom lens design," *Appl. Opt.* **47**, 6088–6098 (2008).
- K. Yamaji, "Design of zoom lenses," in *Progress in Optics VI*, E. Wolf, Ed., pp. 105–170, Elsevier, Amsterdam, The Netherlands (1967).
- F. M. Dickey, *Laser Beam Shaping: Theory and Techniques*, 2nd ed., CRC Press, Boca Raton, Florida (2014).
- F. M. Dickey et al., *Laser Beam Shaping Applications*, CRC Press, Boca Raton, Florida (2005).
- J. E. Greivenkamp, *Field Guide to Geometrical Optics*, SPIE Press, Bellingham, Washington (2004).
- C. Velzel, *A Course in Lens Design*, Springer, Dordrecht, The Netherlands (2014).
- S. Sorgato et al., "Compact étendue-preserving light-mixing optics," *Opt. Express* **23**, A1485–A1490 (2015).
- P. Schreiber et al., "Homogeneous LED-illumination using microlens arrays," *Proc. SPIE* **5942**, 59420K (2005).

Taeshin Kim received his BS degree in mechanical and control engineering from Handong Global University, Pohang, Korea, in 2011. He is currently pursuing a doctoral course in the Department of Advanced Green Energy and Engineering at Handong Global University, Pohang, Korea. His research interests include the design of beam homogenizer and laser applications.

Seungjin Hwang received his BS degree in mechanical and control engineering from Handong Global University, Pohang, Korea, in 2015. He is currently pursuing his doctoral course in the Department of Advanced Green Energy and Engineering at Handong Global University, Pohang, Korea. His research interests include the design of beam homogenizer and high-power systems.

Kyung Hee Hong received his PhD in applied optics from Korea Advanced Institute of Science and Technology, Daejeon, Korea, in 1980. He was a professor of Korea Military Academy, Seoul, Korea. In addition, he was the chairman of optical technology in the Optical Society of Korea. Currently, he is a chair professor at Handong Global University, Pohang, Korea. His research interests include the design of optical systems.

Tae Jun Yu received his PhD in laser physics from Korea Advanced Institute of Science and Technology, Daejeon, Korea, in 2002. He is currently a professor at Handong Global University, Pohang, Korea. His research interests include the development of high-power laser systems.